Electronic structure and effective chemical and magnetic exchange interactions in bcc Fe-Cr alloys

P. A. Korzhavyi* and A. V. Ruban
Department of Materials Science and Engineering, Applied Material Physics, Royal Institute of Technology, SE-100 44 Stockholm, Sweden

J. Odqvist† and J.-O. Nilsson
R&D Centre, Sandvik Materials Technology, SE-811 81 Sandviken, Sweden

B. Johansson
Department of Materials Science and Engineering, Applied Material Physics, Royal Institute of Technology, SE-100 44 Stockholm, Sweden and R&D Centre, Sandvik Materials Technology, SE-811 81 Sandviken, Sweden

(Received 21 July 2008; published 9 February 2009)

Electronic structure calculations are employed in order to investigate the cohesive properties (lattice parameter, enthalpy of formation, and bulk modulus) of random Fe-Cr alloys as a function of composition and magnetic state, as well as to derive the chemical and magnetic exchange interactions of the constituent atoms. The calculations predict certain anomalies in the cohesive properties of ferromagnetic alloys at a concentration of about 7 at % Cr; these anomalies may be related to the changes in Fermi-surface topology that occur with composition in this alloy system. The obtained interatomic interactions are used as parameters in the configurational (Ising) and magnetic (Heisenberg) Hamiltonians for modeling finite-temperature thermodynamic properties of the alloys. We discuss the approximations and limitations of similar modeling approaches, investigate the origin of existing difficulties, and analyze possible ways of extending the theoretical models in order to capture the essential physics of interatomic interactions in the Fe-Cr or similar alloys where magnetism plays a crucial role in the phase stability.

DOI: 10.1103/PhysRevB.79.054202 PACS number(s): 64.75.−g, 71.23.−k, 75.50.Bb

I. INTRODUCTION

Understanding phase equilibria in the body-centered-cubic (bcc) Fe-Cr based alloys is of vital importance for the development of new high-chromium steels. These steels, containing more than 12 wt % Cr, possess good corrosion resistance in very aggressive environments.[1] However, they are known to suffer from a phenomenon called 475 °C embrittlement, which is related to a decomposition of the Fe-Cr solid solution onto the Fe-rich and Cr-rich fractions.[2,3] The decomposition often occurs via the spinodal mechanism.[4–7]

A particular class of steels with almost equal amounts of ferrite (α phase) and austenite (γ phase), so-called duplex stainless steels (DSSs), has rather recently received attention owing to their combination of attractive properties such as toughness, resistance to various types of corrosion, and mechanical strength.[8] To increase the resistance to pitting corrosion the concentration of chromium, molybdenum, and nitrogen is increased but this inevitably leads to microstructural instability. In particular, there is reason to believe that these alloying additions will render also the ferrite in DSS more prone to spinodal decomposition. This is a serious problem for steel makers as well as end users as the upper service temperature, usually 250 °C, is limited by the instability of ferrite. Figure 1 shows an example of the alloy microstructure produced by spinodal decomposition of the α phase (ferrite) in the weld metal of high-chromium duplex stainless steel.[9]

The 475 °C embrittlement problem has motivated extensive experimental studies of the miscibility gap and spinodal decomposition in the Fe-Cr system.[10–17] Stability of bcc Fe-Cr solid solutions has been extensively studied theoretically, mostly by the empirically based Calphad approach.[18–21]

Considerable attention of materials scientists is attracted again to the problem of stability of Fe-Cr based ferrite, now in connection with the development of new types of (thermo)nuclear power reactors.[22] These new studies mostly rely on first-principles calculations and atomistic modeling[23–27] rather than experiments. Although these calculations give some insights into the interplay between magnetism and

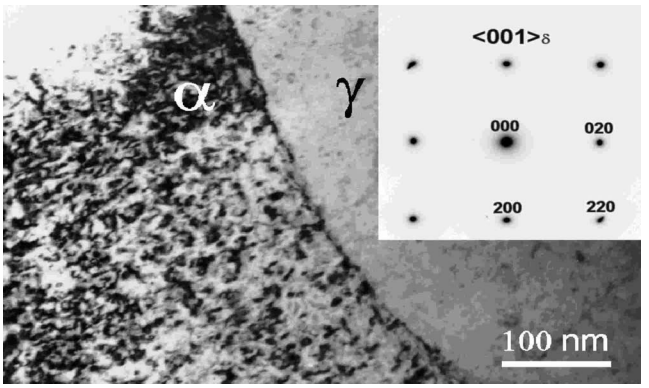

FIG. 1. Modulated contrast due to spinodal decomposition in the ferrite (to the left in the image) obtained using a transmission electron microscope. The contrast is visible in the ⟨001⟩ direction of ferrite (see the diffraction pattern in the inset). Duplex stainless-steel weld metal (Ref. 9) aged for 243 h at 450 °C.

chemical interactions in Fe-Cr alloys, they often ignore some of the important features of the present system: (i) changes in the electronic and magnetic structures of the alloys with composition and temperature; (ii) dependence of the chemical and magnetic interactions on the global magnetic state; (iii) acute concentration dependence of the interactions (in the ferromagnetic state).

The main purpose of the present paper is, therefore, to give a detailed account of the electronic structure and cohesive properties of random Fe-Cr alloys, as well as to show, by means of first-principles perturbation-theory calculations, how the effective chemical and magnetic exchange interactions of atoms in the alloy depend on the concentration and on the global magnetic state. The dependence on magnetic state was addressed in our recent publication.[28] Therefore, in this paper, we focus our attention on the concentration dependence of interatomic interactions. We discuss the origin of these dependencies and analyze their consequences for modeling the finite-temperature properties of Fe-Cr alloys.

II. DETAILS OF CALCULATIONS

A. Electronic structure and total-energy calculations

The locally self-consistent Green's-function (LSGF) method[29,30] has been employed in order to determine the parameters of screened Coulomb interactions,[31–33] as well as to investigate the local environment effects in random bcc Fe-Cr alloys. Total-energy calculations have been done by means of the exact muffin-tin orbital (EMTO) method[34] in the Green's-function formalism which enables one to use the coherent-potential approximation (CPA) (Refs. 35–37) for calculating the electronic structure of substitutionally disordered alloys. The CPA is also employed in this study for modeling the paramagnetic state of the alloys within the disordered local-moment (DLM) approach.[38]

The total energies were calculated in the generalized gradient approximation (GGA) for the exchange-correlation energy,[39] while self-consistent electron densities were obtained within the local-density approximation (LDA).[40] That is, we switched off the gradient corrections to the exchange-correlation potential during the self-consistent calculations, since the GGA is known to overestimate the magnetic moment of bcc iron. The basis functions were expanded up $l_{\max}=3$ in the self-consistent LSGF and EMTO calculations, with expansion to higher orbital quantum numbers for the EMTO full charge-density calculations.[34] Multipole moments of the electron density, up to $l_{\max}^{\mathrm{Mad}}=6$, were determined during the self-consistent calculations of the multipole moment corrections to the Madelung potential and energy.

The on-site screening contributions to the electrostatic potential, v_{scr}^{i}, and energy, E_{scr}, of a random alloy were included in the electronic structure and total-energy calculations in order to take into account the effects of charge transfer between the alloy components, within the single-site density-functional theory approximation:[33]

$$v_{\mathrm{scr}}^{i}=-e^{2}\alpha_{\mathrm{scr}}^{i}\frac{q_i}{S}, \tag{1}$$

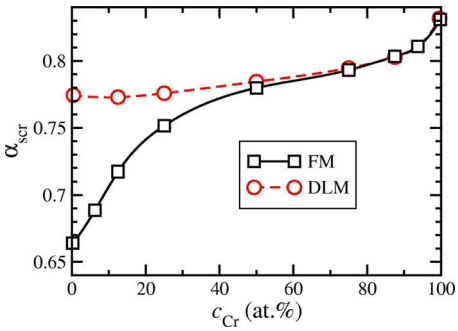

FIG. 2. (Color online) On-site potential screening constant in the FM and DLM states of bcc Fe-Cr alloys.

$$E_{\mathrm{scr}}^{i}=\frac{1}{2}\beta_{\mathrm{scr}}\sum_{i}c_i q_i v_{\mathrm{scr}}^{i}. \tag{2}$$

Here c_i is the concentration and q_i the net charge of the atomic sphere of ith alloy component, S is the Wigner-Seitz radius, and $\alpha_{\mathrm{scr}}^{i}$ and β_{scr} are screening constants. The values of the screening constants have been determined on the basis of LSGF calculations[33] for 512-atom supercells modeling random Fe-Cr alloys with varying composition of Cr. In general, $\alpha_{\mathrm{scr}}^{i}$ is considered to be component-specific; its value can be obtained from the average net charges, $\langle q_i\rangle$, and Madelung potentials, $\langle v_i\rangle$, of the alloy components in a supercell modeling the random alloy:[33]

$$\alpha_{\mathrm{scr}}^{i}=-\frac{S(\langle v_i\rangle-\bar{v})}{e^{2}\langle q_i\rangle}. \tag{3}$$

Here $\bar{v}=\Sigma_i c_i\langle v_i\rangle$ is the total average Madelung potential, which has a small nonzero value even in a highly symmetric cubic crystal due to the contributions arising from nonzero higher-order multipole moments of the electron density. It can be shown that in the case of a binary alloy the on-site screening constants for the two alloy components are equal to each other, i.e., there is only one on-site screening parameter α_{scr} in a binary alloy. In Fig. 2 we show the calculated values of the on-site potential screening constants α_{scr} as a function of concentration in the ferromagnetic (FM) and paramagnetic (DLM) states of bcc Fe-Cr alloys. One can see that the screening constants are very different for the two different magnetic states. The on-site screening constant α_{scr} exhibits a pronounced concentration dependence in the FM state of Fe-rich alloys, whereas in the DLM state the concentration dependence is much weaker. As will be shown below in Sec. III D, the difference in screening parameters may be traced back to the existence of magnetic moments on the Cr atoms in the FM state, as well as to their disappearance in the DLM state, of Fe-rich Fe-Cr alloys.

Let us note that all the previous CPA calculations for Fe-Cr alloys have either completely ignored the screening contribution or treated it very approximately. However, the effective charge transfer between Fe and Cr ($q_{\mathrm{eff}}=|q_{\mathrm{Fe}}-q_{\mathrm{Cr}}|$) is on the order of 0.2 electrons so that the corresponding electrostatic contribution is a sizable part of the mixing energy in this alloy system.

Another screening constant, β_{scr}, is a fitting parameter (on the order of unity) that just renormalizes the electrostatic energy in the single-site CPA calculations in order to make it the same as in the corresponding supercell calculations. (The constant is not exactly equal to 1 because there is an additional electrostatic energy contribution in supercell calculations, as compared to single-site CPA calculations, due to multipole-multipole electrostatic interactions within the alloy configurations that have reduced local symmetry.) The calculated screening constant β_{scr} is found to depend quite strongly on the concentration, as well as on the global magnetic state, of Fe-Cr alloys. For instance, its value in the ferromagnetic state is found to vary from 1.03 to 1.14 upon varying the Cr concentration between the Fe-rich and Cr-rich alloy limits, respectively.

B. Effective chemical interactions

Lavrentiev *et al.*[27] recently applied the structure inversion method (SIM) in order to determine the effective cluster interactions (ECIs) in Fe-Cr alloys from the calculated enthalpies of formation for a set of Fe-Cr superstructures, which were all considered in the FM state. Unfortunately, the interactions of such kind cannot be directly related to the effective interactions that are, for instance, responsible for the atomic short-range ordering effects in random Fe-Cr alloys (at fixed volume, temperature, and composition) as studied experimentally by Mirebeau *et al.*[41] This is so because the interactions derived using SIM are just fitting parameters of a cluster expansion to the enthalpies of formation of a (limited) set of alloys with different compositions, each having a certain atomic configuration and being in a certain magnetic state. As we will see below, the magnetic state and concentration strongly influence the interactions, changing them so dramatically that a transformation of the concentration- and magnetic-state-dependent interactions to the usual concentration- and magnetic-state-independent forms, as assumed in SIM, seems to be a formidable and hardly achievable task.

In this work we calculate the effective cluster interactions using the screened generalized perturbation method (SGPM),[33,42] which is a first-principles generalization of the generalized perturbation method (GPM).[43,44] The approach is based on the force theorem and on the single-site coherent-potential approximation, which are applied within the framework of density-functional theory. The SGPM allows one to calculate the effective cluster interactions in a random alloy having fixed volume and composition and being in a certain magnetic state. An advantage of this method is that any given interaction can be calculated directly and independently from the other interactions. Therefore, the SGPM allows one to investigate the effective chemical interactions in greater detail than is possible using a fitting-based method such as the SIM.

For example, the effective pair interactions are determined within the SGPM as[33,42,44]

$$V_i \equiv V(\mathbf{R}) = V^{\text{one-el}}(\mathbf{R}) + V^{\text{scr}}(\mathbf{R}), \tag{4}$$

where V_i is the SGPM interaction at the ith coordination shell given by a set of vectors $\mathbf{R}$. $V^{\text{one-el}}(\mathbf{R})$ is the one-electron contribution to the SGPM interaction and $V^{\text{scr}}(\mathbf{R})$ is the electrostatic screening contribution,

$$V^{\text{scr}}(\mathbf{R}) = e^2 \alpha_{\text{scr}}(\mathbf{R}) \frac{q_{\text{eff}}^2}{S}. \tag{5}$$

Here $\alpha_{\text{scr}}(\mathbf{R})$ are the *intersite* screening constants.[33,42] Their values for different alloy compositions and magnetic states have been determined from the corresponding supercell calculations. For instance, the values for the first eight coordination shells in $Fe_{75}Cr_{25}$ FM (DLM) random alloy are 0.1256 (0.1244), 0.0542 (0.0443), −0.0091 (−0.0077), −0.0024 (−0.0013), 0.0005 (−0.0006), 0.0013 (0.0), 0.0017 (0.0013), and 0.0015 (0.0007). The screening constants for more distant coordination shells are small and, therefore, the contributions from the corresponding screened Coulomb interactions can be neglected. Multisite interactions contain only one-electron contributions.

III. GROUND-STATE PROPERTIES AND ELECTRONIC STRUCTURE OF RANDOM ALLOYS

A. Lattice parameter and bulk modulus

The lattice parameters of random bcc Fe-Cr alloys have been studied both experimentally[45,46] and theoretically.[25] In general, theory reproduces the experimental lattice parameters with an accuracy of about 1%, which may be considered satisfactory. However, the total change in the lattice parameter in bcc Fe-Cr alloys is less than 1%. Therefore, it is important to discuss the existing discrepancy between theory and experiment in the present system.

The room-temperature experimental lattice parameter monotonously increases with composition, from 2.866 Å in pure Fe to 2.884 Å in pure Cr, but its compositional dependence is strongly nonlinear.[45] Gradient-corrected *ab initio* calculations (our present results are similar to those obtained by Olsson *et al.*[25]) systematically underestimate the lattice parameter of bcc Fe-Cr alloys. The discrepancy is not totally removed even after the atomic vibrations are taken into account (we evaluate the phonon contributions within the Debye-Grüneisen model[47,48] based on the *ab initio* calculated equations of state). Thus for pure iron our calculations give 2.837 Å (static lattice) and 2.857 Å (including phonons, 300 K). The corresponding theoretical values for pure chromium are 2.849 and 2.858 Å.

In order to eliminate the systematic difference between theory and experiment, as well as to focus on the nonlinear behavior of the lattice parameter in the Fe-Cr system, in Fig. 3(a) we plot a relative deviation from Vegard's rule, $(a-\bar{a})/\bar{a}$, where $\bar{a}=(1-c_{\mathrm{Cr}})a_{\mathrm{Fe}}+c_{\mathrm{Cr}}a_{\mathrm{Cr}}$ is the concentration-weighted average of the (experimental or calculated) lattice parameters of pure Fe and Cr, as discussed above.

Both the experimental and calculated (FM) lattice parameters exhibit positive deviations from Vegard's rule for Fe-rich compositions and negative deviations for Cr-rich compositions. (It should be kept in mind that the experimental samples containing less than 70 at. % Cr are in the FM state at room temperature.) Moreover, there is a marked anomaly in the concentration dependence of lattice parameter, which

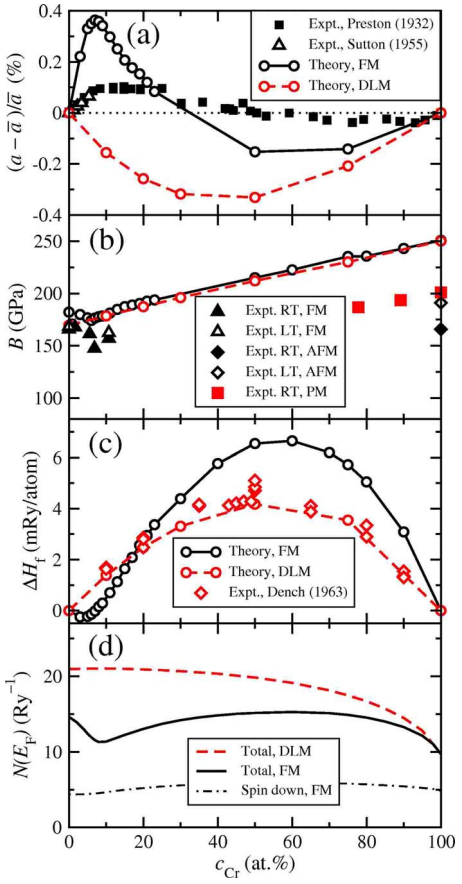

FIG. 3. (Color online) (a) Calculated and experimental (Refs. 45 and 46) deviations of the lattice parameter in bcc Fe-Cr alloys from Vegard's rule. (b) Calculated and experimental (Refs. 49–52) bulk moduli. (c) Calculated and experimental (Ref. 53) enthalpy of formations. (d) Calculated density of states at the Fermi level in the FM and paramagnetic (DLM) Fe-Cr alloys.

is present in both the experimental and the calculated (FM) data. The initial steep slope of the concentration dependence (which suggests a relatively large effective size of a Cr impurity in pure Fe) changes abruptly to a lower value corresponding to a smaller size of the Cr atoms added to Fe-Cr alloys in excess of 7 at % Cr. The lattice parameter of Fe-Cr alloys in the DLM state exhibits a regular concentration dependence, with negative deviations from Vegard's rule in the whole concentration range.

Figure 3(b) shows the calculated bulk modulus of random bcc Fe-Cr alloys together with available experimental data.[49–52] The theoretical values have been obtained from the calculated equations of state for FM alloys on a static lattice (i.e., without phonon contributions). The plotted experimental bulk moduli include the data for ferromagnetic alloys at room temperature (RT) and at a low temperature (LT) of 77 K,[49] the RT data for paramagnetic Cr-rich Fe-Cr alloys,[50] an experimental estimate of the RT bulk modulus of "paramagnetic" Cr,[50,51] as well as the RT and LT data for antiferromagnetic Cr.[51,52]

The calculated bulk moduli of Fe-rich alloys, in the FM state, exhibit an anomaly with a sharp minimum at 6 at % Cr. Experimental data for Fe-rich Fe-Cr alloys[49] suggest a similar nonmonotonous concentration dependence, with a local minimum at 7 at % Cr. The calculated concentration dependence of the bulk modulus for Fe-Cr alloys in the DLM state is monotonous.

B. Enthalpy of formation

The calculated enthalpies of formation of Fe-Cr alloys, in the FM state as well as in the DLM state, are presented in Fig. 3(c). Note that standard states of Fe are different for the FM and DLM curves; the calculated energy difference between the FM and DLM configurations of pure Fe is about 15 mRy/atom. Both the FM and DLM calculations for pure Cr converge to a nonmagnetic solution, which is the standard state for both calculated curves. The experimental enthalpy of formation has been determined relative to Fe and Cr in their respective high-temperature paramagnetic states.[53] Naturally, good agreement is found between the experimental enthalpies of formation of paramagnetic Fe-Cr alloys[53] and our DLM results [see Fig. 3(c)].

In this respect, it should be mentioned that the experimental enthalpy of formation, measured in the paramagnetic state, cannot be compared to the enthalpies of formation obtained as a result of high-temperature Monte Carlo (MC) simulations by Lavrentiev *et al.*[27] This is so because the effective cluster interactions in Ref. 27 were obtained from the total energies of Fe-Cr superstructures *in the ferromagnetic state*. Indeed, the atomic configuration in the MC simulation at a high enough temperature approaches that of a random alloy. Therefore, as $T\rightarrow\infty$, their MC computed enthalpy of formation should approach the enthalpy of formation of random Fe-Cr alloys in the FM state. This is why the enthalpies of formation calculated by Lavrentiev *et al.*[27] for Fe-Cr alloys at 1800 K exhibit exactly the same anomalous mixing behavior, with the sign change of the enthalpy of formation in the Fe-rich region, as our calculations predict for random FM alloys [the black solid curve in Fig. 3(c)]. Note also that one experimental point (the one that is supposed to lie at 10 at % Cr) has been displaced toward more Cr-rich compositions by Lavrentiev *et al.*[27] in Fig. 5 of their paper.

Real Fe-Cr alloys are, of course, in the paramagnetic state at 1800 K, and their enthalpy of formation [the dashed curve and rhombi in Fig. 3(c)] is not expected to exhibit any anomalies in the Fe-rich region. The existence of a mixing tendency in Fe-rich Fe-Cr alloys is a feature, as now well understood,[25] of the FM state and must disappear above the Curie temperature.

Let us also note, in passing, that in the Fe-rich region the effect of atomic short-range order (ASRO) is small due to the fact that the energy contribution from the ASRO of ordering type is proportional to c^2, where c is the concentration of the minority element in the alloy ($c\equiv c_{Cr}$ in our case). At the same time, the contribution from the ASRO of clustering type is proportional to $c(1-c)$, so it gives quite substantial contribution close to the equiatomic composition, as well as in the Cr-rich region. This means that the MC results of Ref. 27 for 1800 K should underestimate the enthalpy of formation of the ferromagnetic random alloy due the substantial amount of ASRO of clustering type in their simulation box at that temperature.

Our results for the thermodynamic properties are, of course, similar to those obtained earlier by Olsson and co-workers[24,25] who also used the EMTO method in combination with full-potential supercell calculations. However, there are slight numerical differences between the two sets of EMTO results, which are caused by the more sophisticated treatment of the electrostatic screening contributions in the present study, as has been described in Sec. II A. In particular, our calculations yield a value of −0.25 mRy (−3.3 meV) for the enthalpy of formation of Fe-Cr alloys in the FM state at the minimum located near 3 at % Cr, while the enthalpy of formation is calculated to change sign close to 7 at % Cr. Ironically, these results are in very good agreement with the above-mentioned MC results by Lavrentiev *et al.*[27]

C. Density of states and Fermi surface

Thermodynamic properties of any material derive from its electronic structure.[54] Metallic alloys are no exception: the electronic structure is well known to play an important role in the structural stability of metallic alloys,[55–58] as well as to affect other physical properties of metals near the points where the electronic structure undergoes a discontinuous change.[59–65] Let us now consider how the electronic structure of Fe-rich Fe-Cr alloys (in the FM state) evolves with chemical composition in order to see the origin of the anomalous concentration dependence of their thermodynamic properties. An abrupt discontinuity in the slope of concentration dependence of the density of states (DOS) at the Fermi level has been noticed in the CPA-based electronic structure calculations[24,25,66] of random Fe-Cr alloys. As Fig. 3(d) shows, the discontinuity occurs only in the spin-up channel[25] and is located near the concentration (7 at % Cr) at which the thermodynamic properties of ferromagnetic alloys exhibit the anomalous behavior [see Figs. 3(a)–3(c)]. Hereafter, the majority-spin channel of Fe in the FM state of Fe-Cr alloys is referred to as the "spin-up" channel. Chromium tends to align its magnetic moment antiparallel to that of iron, therefore, the majority-spin channel for Cr is the "spin-down" channel. The reader is referred to paper by Olsson *et al.*[25] for more details about the DOS of Fe-Cr alloys.

A simple relationship between the DOS at the Fermi level $N(E_F)$ and the thermodynamic stability (against spinodal decomposition) of a random solid solution can readily be established using arguments based on the rigid-band model and Fermi-surface topology.[67] Although the rigid-band model is only approximately valid even for *sp*-valent metal alloys,[68] the simple relationship [between $N(E_F)$ and the second concentration derivative of total energy] has been found to make qualitatively correct predictions of spinodal instability even in the case of Fe-Cr alloys.[25] This result is surprising because, as is well known and will once again be illustrated below, the electronic structure of *d*-transition metal alloys such as Fe-Cr does not exhibit a rigid-band behavior.

In Fig. 4 the calculated densities of electron states on Fe and Cr atoms in random alloys $Fe_{98}Cr_{02}$ and $Fe_{90}Cr_{10}$ are shown. An important observation is that a shoulder, which is located at E_F in the Fe-projected spin-up DOS of $Fe_{98}Cr_{02}$ alloy, disappears in the DOS of $Fe_{90}Cr_{10}$ alloy. At the same time there is an increase in the Cr-projected spin-up DOS at Fermi level upon changing the Cr concentration from 2 to 10 at %. Other important observations are that both the Fe- and Cr-projected DOS, in the spin-down channel, have deep minima at the Fermi level and that their shape in the vicinity of E_F depends very little on the alloy composition.

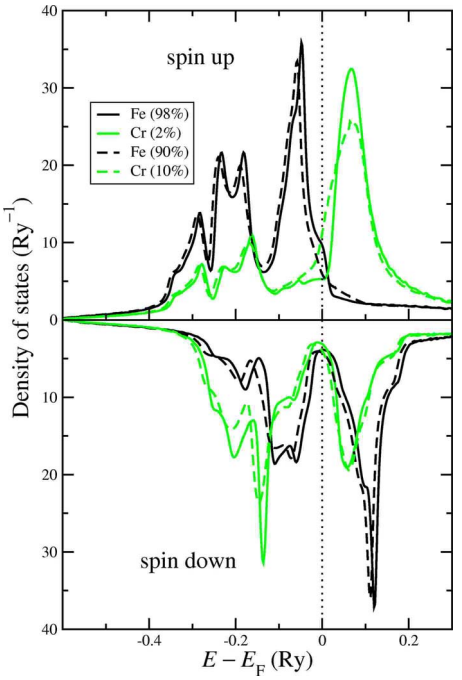

FIG. 4. (Color online) Calculated atom-projected densities of electron states in random bcc alloys $Fe_{98}Cr_{02}$ and $Fe_{90}Cr_{10}$ in the FM state.

Figure 5 shows the Fe- and Cr-projected DOSs in the *paramagnetic* (DLM) state of random bcc alloys $Fe_{98}Cr_{02}$ and $Fe_{90}Cr_{10}$. The most striking feature of the DLM densities of states is that the Fe-projected DOS in the minority-spin channel (labeled spin down in Fig. 5) is aligned in energy with the Cr-projected DOS (the latter is the same in both spin channels as the magnetic moment on Cr vanishes in the DLM state). Furthermore, due to the presence of magnetic disorder, all the DOSs look somewhat smeared out, as compared to the FM case presented in Fig. 4. One also notices that the DLM densities of states are almost insensitive to the Cr concentration from 2 to 10 at %.

The Fermi-surface (FS) evolution with composition in ferromagnetic Fe-rich Fe-Cr alloys is presented in Fig. 6. The figure shows FS cross sections by the (001) plane, visualized using the calculated density of electron states in reciprocal space (Bloch spectral function) for the two spin channels (up and down) at the Fermi energy.[69,70] Our calculations indicate that the change in composition from 0 to 15 at % Cr has no significant effect on the Fermi surface of the Fe-Cr alloys in the spin-down channel. This is a consequence of the fact that the spin-down electron states of Fe and Cr in the FM Fe-Cr alloys are almost perfectly aligned in energy in the vicinity of E_F (see Fig. 4). Therefore, electron scattering off the Fe and Cr atoms is very coherent in this spin channel so that the electron states near the Fermi energy preserve their band character (see Fig. 7).

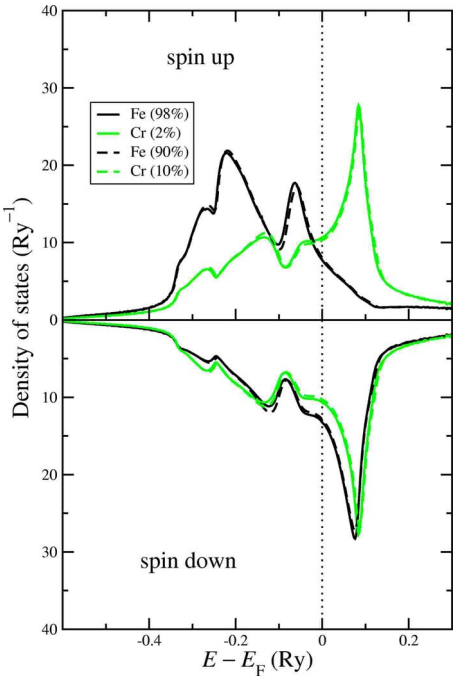

FIG. 5. (Color online) Calculated atom-projected densities of electron states in random bcc alloys $Fe_{98}Cr_{02}$ and $Fe_{90}Cr_{10}$ in the paramagnetic (DLM) state.

In sharp contrast, the FS for the spin-up electron states undergoes dramatic changes in a narrow concentration interval between 5 and 10 at % Cr: the hole arms (multiconnected parts embracing the first Brillouin zone),[71–78] as well as the hole pockets (located at the vortices, points H, **k** ={100} of the Brillouin zone),[79,80] of the spin-up FS of pure Fe completely disappear from the Fermi surface when the alloy concentration reaches 10 at % Cr. Only the central part of the spin-up FS (enclosing electron states) does preserve its band character in the 10 at % Cr alloy.

The hole pockets at points H close up in a rigid-band manner with increasing the Cr concentration as if the holes in the spin-up (majority) channel of Fe were filled up by chromium spin-up (minority) electrons. Figure 7 shows that these pockets become closed at approximately 5 at % Cr where the corresponding states at the Fermi energy near points H can still be distinguished as band states. At a higher concentration of 10 at % Cr the band structure near these points becomes "smeared out." Because of a strong difference between the scattering properties of the Fe and Cr ionic potentials in the spin-up channel, the electron spectrum loses its band character and becomes imaginary in a certain domain of wave vectors and energies near the Fermi energy. In Fig. 7(c) this domain is seen as a gray "cloud" of states at energies between 0.0 and 0.1 Ry. The states within the cloud have lost their band character to form a break in the $E(\mathbf{k})$ dependence. Thus, strong scattering induces a "band gap" in the spin-up electronic spectrum of FM Fe-Cr alloys. One can anticipate that the presence of a scattering-induced band gap in one spin channel must affect spin-dependent transport properties of FM Fe-Cr alloys. For example, the electrical conductivity in the spin-up channel may be expected to become much lower than in the spin-down channel.

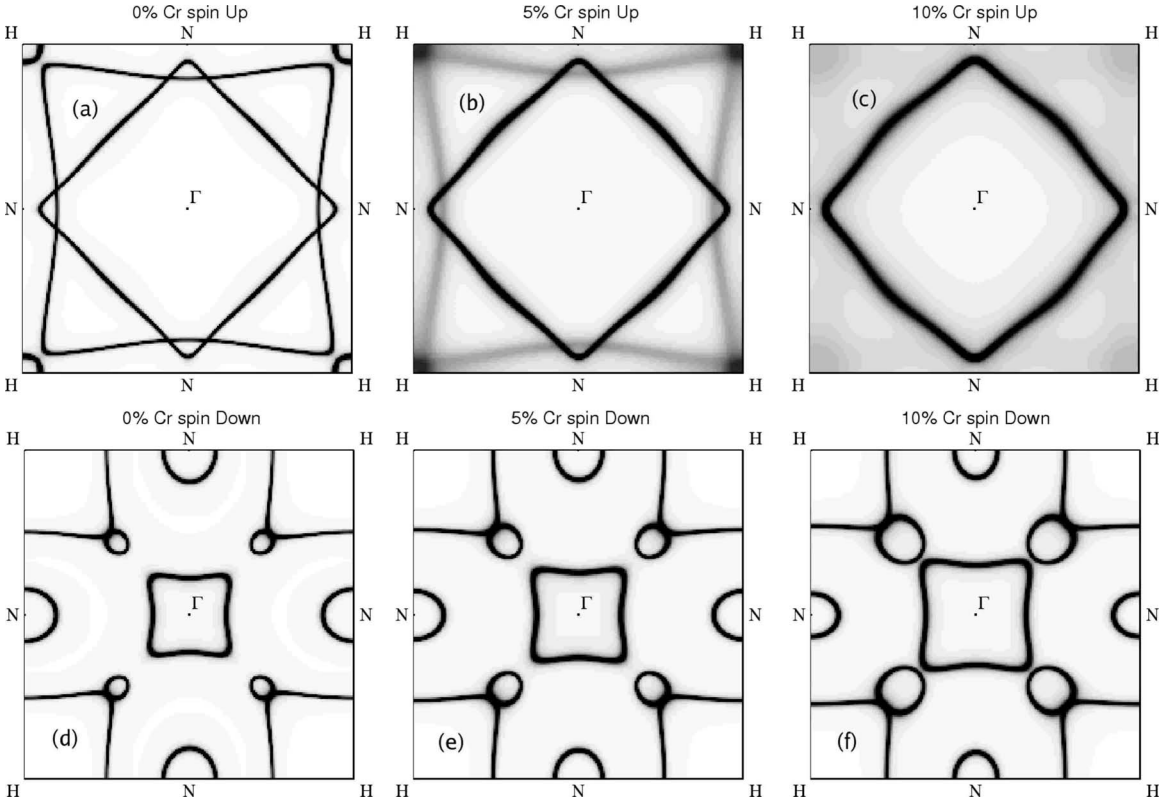

FIG. 6. Evolution of the Fermi surface of bcc Fe-Cr alloys with composition.

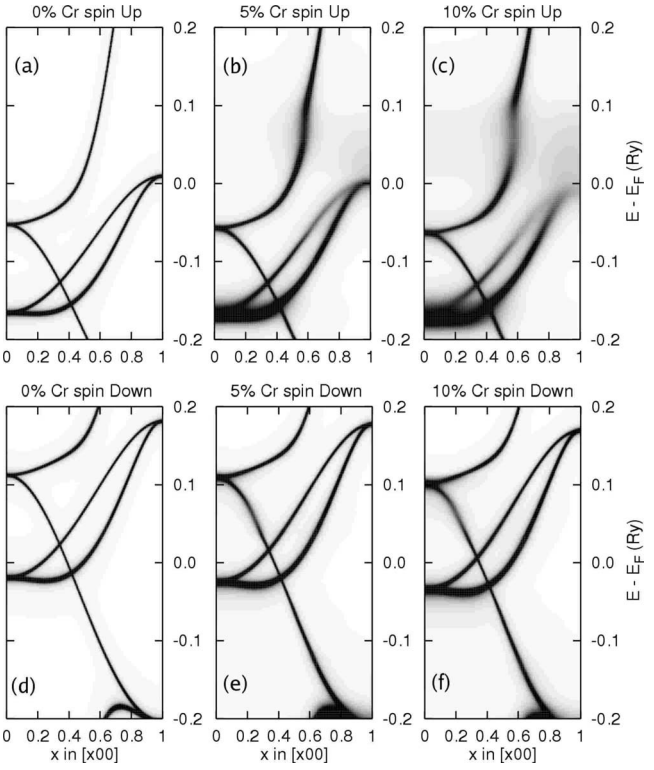

FIG. 7. Evolution of the electronic spectrum of bcc Fe-Cr alloys with composition.

D. Magnetic moments

The results to be presented in this section have been calculated at a fixed lattice parameter of $a_0=2.875$ Å, which is the average of the room-temperature lattice parameters of bcc Fe and bcc Cr. We have checked, however, that the volume dependence of magnetic moments is weak and can safely be neglected in the present case, also taking into account the small difference between the lattice parameters of bcc Cr and Fe. The calculation procedure to be described below in this section yields *configuration-averaged* values of magnetic moments, which are suitable for making comparisons with experiment. Fluctuations of magnetic moments, due to local environment effects, will be considered separately in Sec. V.

1. Ferromagnetic state

In the practice of electronic structure calculations the spin moment on an individual atom is usually associated with the imbalance between the spin-up and spin-down components of the electron density integrated over the spatial region (Wigner-Seitz cell or sphere) that is ascribed to that particular atom. This procedure becomes ambiguous when the crystal is made of more than one type of atom (or its structure has inequivalent sites) because the electron densities of neighboring atoms in the crystal overlap. Only the total magnetic moment of all the atoms in the primitive cell of the crystal is unambiguously defined. In order to determine the individual magnetic moments of the Fe and Cr atomic species (M_{Fe} and M_{Cr}, respectively) we use a standard procedure for calculation of partial molar properties from the concentration dependence of an extensive thermodynamic quantity.[81] In this particular case, this quantity is the total magnetic moment of the alloy (normalized per atom), $m_{\mathrm{tot}}(c)$, considered as a function of concentration c. It may be represented as the weighted sum of individual magnetic moments of the atomic species, Fe and Cr,

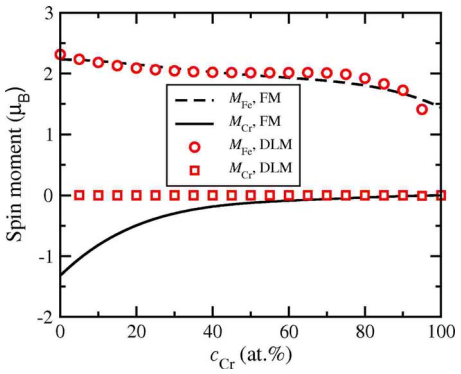

FIG. 8. (Color online) Calculated concentration dependencies of the magnetic moments on the Fe and Cr atoms in the ferromagnetic (lines) and paramagnetic (symbols) states of Fe-Cr alloys.

$$m_{\mathrm{tot}} = (1-c)M_{\mathrm{Fe}} + cM_{\mathrm{Cr}}. \tag{6}$$

Hereafter we omit to explicitly show the concentration dependence of magnetic moments $m_{\mathrm{tot}}(c)$, $M_{\mathrm{Fe}}(c)$, and $M_{\mathrm{Cr}}(c)$. The variation in total magnetization with the alloy composition may be represented as a result of substitution of a chromium atom for an iron atom

$$\frac{dm_{\mathrm{tot}}}{dc} = -M_{\mathrm{Fe}} + M_{\mathrm{Cr}}. \tag{7}$$

Combining Eqs. (6) and (7) one can determine the magnetic moments of the Fe and Cr atoms as

$$M_{\mathrm{Fe}} = m_{\mathrm{tot}} - c\frac{dm_{\mathrm{tot}}}{dc},$$

$$M_{\mathrm{Cr}} = m_{\mathrm{tot}} + (1-c)\frac{dm_{\mathrm{tot}}}{dc}. \tag{8}$$

Their concentration dependencies are shown in Fig. 8 as the dashed (dot-dashed) line for Fe (Cr). The negative sign of the Cr magnetic moment reflects the fact that, in the ferromagnetic state of random bcc Fe-Cr alloys, the Cr magnetic moment is aligned antiparallel to the Fe magnetic moment, as well as to the global magnetization vector.

2. Paramagnetic state

The total magnetic moment averages to zero in the paramagnetic state. Therefore, the procedure that was applied to determine the atomic magnetic moments the FM state, Eqs. (6) and (7), should be modified in order to handle this new situation. Paramagnetic moments are the microscopic parameters that describe the magnitude of fluctuations of the spin moment orientation in the paramagnetic state. A natural definition of the (para)magnetic moment, associated with the

given atom, may be obtained if one considers the change in total magnetization of the system upon a reversal of the magnetic-moment orientation on that particular atom.

In our calculations this magnetization reversal process was modeled by flipping the spin moment direction of a small fraction δ of, say, Fe$\downarrow$ (thereby creating a small spin imbalance 2δ) and calculating the deviation of the total magnetic moment m_{tot} from zero for this new spin structure. Thus, in order to calculate the magnetic moment of Fe in the paramagnetic state of the $Fe_{60}Cr_{20}$ alloy, we calculated the magnetic moment per atom, m_{tot}, for the following spin structure: $Fe\uparrow_{30+\delta}Fe\downarrow_{30-\delta}Cr\uparrow_{20}Cr\downarrow_{20}$. The paramagnetic moment of Fe is then obtained as

$$M_{\mathrm{Fe}} = \frac{m_{\mathrm{tot}}}{2\delta}. \tag{9}$$

The paramagnetic moment of Cr may be calculated using the same procedure. In the calculations we used $\delta=0.5$ at % if the concentration of the component in question was 5 at %, $\delta=1$ at % if the concentration of the component in question was 10 at %, and $\delta=2$ at % in all the other cases.

The calculated concentration dependencies of the Fe and Cr magnetic moments in the paramagnetic state are shown in Fig. 8 as open symbols (circles and squares, respectively). The values of the Fe and Cr magnetic moments in the FM state are also shown in Fig. 8 for comparison.

Two important observations are the following:

(i) The magnetic moment of Cr vanishes in the paramagnetic configuration of the bcc Fe-Cr alloys. A similar behavior of the Cr magnetic moments in paramagnetic fcc Fe-Cr-Ni based alloys has been obtained in *ab initio* calculations.[82,83] We note that the paramagnetic configurations have been considered at $T=0$ K in this as well as in the previous studies, so that the temperature-induced *longitudinal* fluctuations[84–87] of magnetic moments are ignored here.

(ii) The magnetic moments on iron atoms in the paramagnetic and ferromagnetic states of bcc Fe-Cr alloys have very similar values. This result shows that it is not unreasonable to view the ferromagnetic-to-paramagnetic transition in iron as occurring by disordering the local moments of individual Fe atoms.

The compositional dependence of the iron magnetic moment in the paramagnetic state is somewhat stronger than that in the ferromagnetic state. This dependence is, nevertheless, smooth and continuous. The magnetic moment of Fe is close to 2 μ_B for the alloy concentrations up to 80 at % Cr. A comparison of Figs. 2 and 8 allows one to explain the fact of strong concentration dependence of the on-site screening constant α_{scr} in bcc Fe-Cr alloys. Formation of a local spin moment on Cr impurities in the Fe-rich matrix may be viewed as localization of valence electrons, which reduces the number of valence electrons and makes the screening less efficient (a lower value of α_{scr} corresponds to a larger effective screening radius). On the Cr-rich end of the alloy compositions, the decreasing magnetic moment on Fe impurities produces a corresponding increase of the on-site screening constant as a function of Cr concentration. Thus, the observed screening anomalies are direct consequences of the quantum-mechanical relationship between spin and valence.[88]

IV. EFFECTIVE CHEMICAL INTERACTIONS

The effective chemical interactions are microscopic parameters of configurational Ising Hamiltonian, which is the basis for statistical thermodynamic modeling of substitutional alloys on a fixed lattice. The effective chemical interactions characterize the tendency of an alloy toward ordering or phase separation. For instance, the effective pair interaction at a given coordination shell is the energy preference of having pairs of unlike atoms to having pairs of like atoms at a distance of the coordination shell radius. Thus, if the pair interaction energy is positive (negative), ordering (separation) should occur on the corresponding coordination shell at sufficiently low temperatures.

The effective chemical interactions in the Fe-Cr alloys were first obtained theoretically by Hennion[89] who used for this purpose the GPM (Ref. 43) implemented in the framework of tight-binding Hartree-Fock theory. Mirebeau *et al.*[41] predicted that there should be ordering in the FM state of Fe-rich alloys up to 25 at % of Cr, and later this theoretical result was confirmed experimentally in the diffuse-neutron-scattering measurements; however, the transition from ordering to clustering behavior was found at about 10 at % Cr. A more detailed discussion of this issue is given in Ref. 28.

More accurate first-principles GPM calculations of the effective interactions in equiatomic Fe-Cr alloys were performed later by Turchi *et al.*,[90] and the results appeared to be in excellent agreement with those deduced from the anomalous x-ray-scattering data using the inverse Monte Carlo method.[91] In a subsequent work Turchi *et al.*[23] determined the effective pair interactions in the whole concentration range and used them in the first *ab initio* evaluation of the miscibility gap on a fixed bcc lattice. Their results were in reasonable agreement with experimental data. However, if the results for Cr-rich compositions can probably be trusted, in the case of Fe-rich compositions they are questionable since all the calculations were spin unpolarized (i.e., assumed a nonmagnetic state of the alloys).

In the present work we use the SGPM (Refs. 33 and 42) for obtaining the effective cluster interactions, as a function of concentration and magnetic state, in bcc Fe-Cr alloys. This issue is very important because such interactions are directly related to interatomic potentials, which are being intensively developed for the Fe-Cr alloy system in connection with a strong need for modeling such alloys using large-scale molecular-dynamics simulations.[92–101] Of course, the SGPM, being based on the single-site mean-field approximation, has its own limitations and errors.[102] We will see below that it presents a *simplified* version of real physics. Nevertheless, this simplified picture is qualitatively correct and, therefore, it gives a very important insight into the physics of interactions in Fe-Cr alloys.

Let us first discuss the effective pair interactions (EPIs) (all the data presented here have been obtained at a fixed lattice spacing of 2.875 Å, regardless of composition or magnetic state of Fe-Cr alloys, thereby neglecting the effect

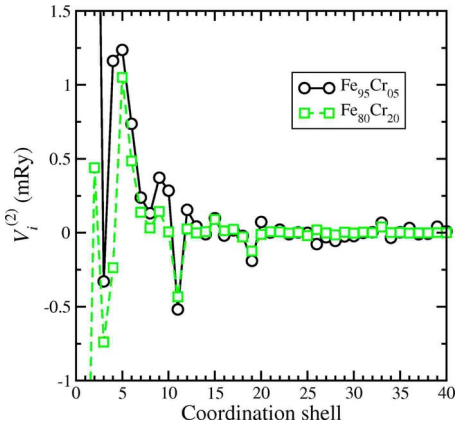

FIG. 9. (Color online) Effective pair interactions in $Fe_{95}Cr_{05}$ and $Fe_{80}Cr_{20}$ alloys in the FM state.

of volume, which is anyway small in this system). In Fig. 9 we show the calculated EPIs for $Fe_{95}Cr_{05}$ and $Fe_{80}Cr_{20}$ alloys in the FM state. A scale is chosen such as to show the behavior of a long-range tail of the EPI; therefore, the EPI at the first two coordination shells for $Fe_{95}Cr_{05}$ ($V_1^{(2)}=14.8$ and $V_2^{(2)}=4.8$ mRy) and the nearest-neighbor EPI for $Fe_{80}Cr_{20}$($V_1^{(2)}=-2.9$ mRy) cannot be seen in the figure. It is clear that interactions decay reasonably fast with the distance. At the same time one notices that interactions at 9th and 19th coordination shells are strong relative to their "neighbors." These EPIs correspond to vectors $\mathbf{R}=(3,3,3)$ and (4,4,4) (in units of $a/2$, where a is the lattice constant), i.e., to vectors aligned in the close-packed direction.

This is, in fact, a very common situation for the EPI in metallic alloys, independently of the underlying lattice: the strongest EPIs for distant coordination shells are usually found for the vectors that are aligned in the close-packed direction. Exactly the same rule applies to multisite interactions: the strongest multisite interactions are usually those that correspond to atomic clusters aligned in the closed-packed direction. In Tables I and II we show the values of selected three-site and four-site effective interactions for the $Fe_{95}Cr_{05}$ and $Fe_{80}Cr_{20}$ alloys in the FM state. The clusters are designated by vectors connecting the first site (positioned at the origin) to the other sites that belong to the cluster. Also specified in the tables are the coordination shell index (CSI), which gives the coordination shell number for every edge of the cluster (triangle or tetrahedron), as well as the total number of clusters of the given type (degeneracy).

The clusters aligned along the closed-packed direction are three-site cluster {(1,1,1),(2,2,2)} and four-site cluster {(1,1,1),(2,2,2),(3,3,3)}. Indeed, our calculations show that the magnitudes of interactions corresponding to these clusters are comparatively large. Of course, it is not only the magnitude that plays a decisive role in the configurational energetics: the number of clusters (degeneracy) is also important. Anyway, it is clear that there are quite many three-site and four-site interactions that are strong enough to be necessarily taken into account when describing the thermodynamics of the present alloy system.

It is obvious from the results presented above that there is quite strong concentration dependence of the effective cluster interactions, which is a natural consequence of the changes in the electronic and magnetic structures with composition of Fe-Cr alloys. In order to illustrate this connection, we show in Fig. 10 the strongest EPI at the first coordination shell, as well as the two strongest three-site interactions, $\{(1,1,1),(1,1,\bar{1})\}$ and {(1,1,1),(2,2,2)}, one four-site interaction {(1,1,1),(2,2,2),(3,3,3)}, and one five-site interaction {(1,1,1),(2,2,2),(3,3,3),(4,4,4)} calculated in the whole compositional range of Fe-Cr alloys. The EPI is shown for three different magnetic states: FM, DLM,[28,42] and nonmagnetic (NM).

TABLE I. Three-site interactions in $Fe_{95}Cr_{05}$ and $Fe_{80}Cr_{20}$ alloys in the FM state.

$\{\mathbf{R}_1,\mathbf{R}_2\}$	CSI	No.	$Fe_{95}Cr_{05}$	$Fe_{80}Cr_{20}$
$\{(1,1,1),(1,1,\bar{1})\}$	1 1 2	36	0.819	1.427
$\{(1,1,1),(1,\bar{1},\bar{1})\}$	1 1 3	36	−0.231	−0.414
{(1,1,1),(2,2,2)}	1 1 5	12	3.113	1.443
$\{(1,1,1),(\bar{2},0,0)\}$	1 2 4	72	0.256	−0.940
{(2,0,0),(0,2,0)}	2 2 3	36	−0.414	−0.077
$\{(2,0,0),(\bar{2},0,0)\}$	2 2 6	9	0.556	−0.040
$\{(1,1,1),(\bar{2},2,0)\}$	1 3 4	144	0.005	−0.022
$\{(1,1,1),(\bar{2},\bar{2},0)\}$	1 3 7	72	0.064	−0.007
{(2,0,0),(0,2,2)}	2 3 5	72	0.069	−0.050
$\{(2,0,0),(\bar{2},2,0)\}$	2 3 8	72	0.018	−0.003
{(2,2,0),(2,0,2)}	3 3 3	24	−0.048	0.022
$\{(2,2,0),(2,\bar{2},0)\}$	3 3 6	36	−0.065	0.017
$\{(1,1,1),(3,\bar{1},\bar{1})\}$	1 4 5	72	0.192	−0.020
$\{(1,1,1),(\bar{3},1,1)\}$	1 4 6	72	0.071	0.044
$\{(1,1,1),(\bar{3},1,\bar{1})\}$	1 4 8	144	0.025	0.000
{(2,0,0),(1,3,1)}	2 4 4	72	0.047	0.024
$\{(2,0,0),(\bar{1},3,1)\}$	2 4 7	144	−0.040	0.007
{(2,2,0),(1,1,3)}	3 4 4	108	0.059	−0.018
$\{(2,2,0),(1,\bar{1},3)\}$	3 4 7	144	0.004	0.011
$\{(3,1,1),(1,3,\bar{1})\}$	4 4 5	72	0.036	0.019
$\{(3,1,1),(\bar{1},3,1)\}$	4 4 8	144	−0.002	0.007
$\{(1,1,1),(2,\bar{2},\bar{2})\}$	1 5 7	72	0.121	−0.022
$\{(1,1,1),(\bar{2},\bar{2},\bar{2})\}$	1 5 11	24	0.133	0.368

First of all one can see that values and the behavior of $V_1^{(2)}$ are substantially different in the FM state from those in the DLM or NM states. In the latter two cases the interactions are weaker and change only slightly with alloy composition, while in the FM state all the ECI exhibit very strong concentration dependencies for the Fe-rich compositions. The nearest-neighbor EPI, $V_1^{(2)}$, is large and positive in this region, in the FM state, which corresponds to atomic ordering and should lead to alloying between Fe and Cr. This is the effect predicted by Hennion[89] long time ago; it can also be seen from the calculated enthalpy of formation of Fe-Cr alloys in the FM state [Fig. 3(c)]. In the DLM state, the nearest-neighbor interaction is practically independent of

TABLE II. Four-site interactions in $Fe_{95}Cr_{05}$ and $Fe_{80}Cr_{20}$ alloys in the FM state.

$\{\mathbf{R}_1,\mathbf{R}_2,\mathbf{R}_3\}$	CSI	No.	$Fe_{95}Cr_{05}$	$Fe_{80}Cr_{20}$
$\{(1,1,1),(2,0,0),(1,1,\bar{1})\}$	1 1 2 2 1 1	24	−0.381	0.625
$\{(1,1,1),(2,0,0),(1,\bar{1},\bar{1})\}$	1 1 2 3 1 1	24	0.793	0.802
$\{(1,1,1),(1,1,\bar{1}),(\bar{1},1,1)\}$	1 1 1 2 2 3	96	−0.815	0.393
$\{(1,1,1),(\bar{1},1,\bar{1}),(1,\bar{1},\bar{1})\}$	1 1 1 3 3 3	32	0.110	−0.118
$\{(1,1,1),(1,1,\bar{1}),(\bar{1},\bar{1},1)\}$	1 1 1 2 3 5	96	0.580	−0.079
$\{(1,1,1),(\bar{1},1,\bar{1}),(2,0,0)\}$	1 1 2 3 1 4	192	0.115	0.009
$\{(1,1,1),(1,1,\bar{1}),(\bar{1},3,1)\}$	1 1 4 2 3 5	192	−0.072	−0.041
$\{(1,1,1),(2,2,2),(3,3,3)\}$	1 5 11 1 5 1	8	2.414	1.635
$\{(1,1,1),(\bar{1},\bar{1},\bar{1}),(2,0,0)\}$	1 1 2 5 1 4	96	0.801	−0.249
$\{(1,1,1),(\bar{1},1,\bar{1}),(2,2,0)\}$	1 1 3 3 1 4	96	−0.394	−0.041
$\{(1,1,1),(\bar{1},\bar{1},\bar{1}),(2,\bar{2},0)\}$	1 1 3 5 4 4	96	0.111	−0.059
$\{(1,1,1),(1,1,\bar{1}),(3,1,\bar{1})\}$	1 1 4 2 2 3	192	0.091	−0.152
$\{(1,1,1),(1,1,\bar{1}),(1,1,3)\}$	1 1 4 2 2 6	96	0.091	0.132
$\{(1,1,1),(1,1,\bar{1}),(\bar{1},3,1)\}$	1 1 4 2 3 5	192	−0.072	−0.041
$\{(1,1,1),(\bar{1},1,\bar{1}),(1,3,\bar{1})\}$	1 1 4 3 3 3	96	−0.134	0.104
$\{(1,1,1),(\bar{1},1,\bar{1}),(3,1,\bar{1})\}$	1 1 4 3 3 6	192	−0.047	−0.003
$\{(1,1,1),(\bar{1},\bar{1},\bar{1}),(3,\bar{1},\bar{1})\}$	1 1 4 5 5 6	96	0.306	0.084
$\{(1,1,1),(1,1,\bar{1}),(4,0,0)\}$	1 1 6 2 4 4	96	−0.019	−0.107

concentration and is negative everywhere, which means that Fe and Cr atoms tend to avoid each other at the nearest-neighbor distance in the paramagnetic DLM state of the alloy, thereby inducing a phase separation. This result is again in accordance with the calculated enthalpies of formation for Fe-Cr alloys in the paramagnetic DLM state [Fig. 3].

The chemical interactions in the NM state of Fe-Cr alloys are shown in Fig. 10 for the sake of comparison only. The NM state is too crude a model for the paramagnetic state of Fe-rich Fe-Cr alloys, since, as has been noted above, the Fe atoms retain substantial magnetic moments in the paramagnetic state above the Curie temperature.[103] One can see that the effective interaction within the first coordination shell is actually positive in the NM state up to 60 at % Cr, which contradicts the existing experimental data about ASRO in the paramagnetic alloys.[91]

The origin of strong concentration dependence of the ECI in Fe-rich Fe-Cr alloys is now well understood.[26] Cr atoms interact antiferromagnetically with each other and with the Fe atoms. Therefore, as soon as two or more Cr impurities in bcc Fe become nearest neighbors, there will be a frustration; as a result the Cr atoms decrease (or completely lose) their magnetic moments, thereby altering the magnetic and chemical interactions between Fe and Cr. In Fig. 11 we show the concentration dependence of the local magnetic moment on Cr m_{Cr} (here, in contrast to M_{Cr} discussed in Sec. III D, the local moment is defined as the integral spin imbalance inside the Cr atomic sphere) and the magnetic exchange interaction parameters of the Heisenberg Hamiltonian at the first coordination shell, J_1, in the FM state. It is clear that the concentration dependencies of $J_1^{\text{Fe-Cr}}$ and m_{Cr} are very similar to that of $V_1^{(2)}$.

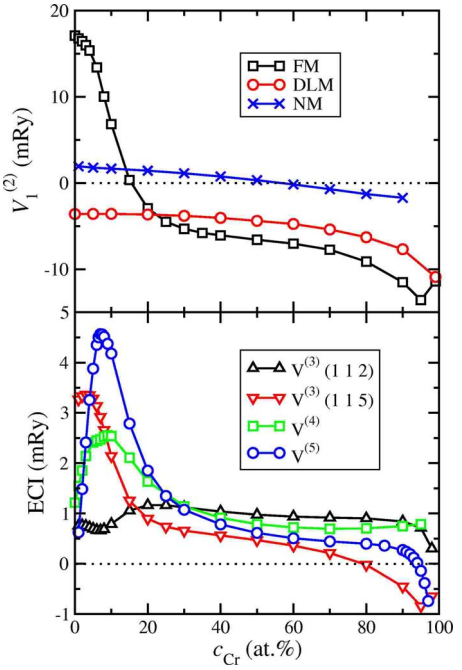

FIG. 10. (Color online) Top panel: EPI at the first coordination shell in three different states: FM, paramagnetic (DLM), and NM. Bottom panel: The strongest three-site, $V^{(3)}(112) = V^{(3)}(\{(1,1,1),(1,1,\bar{1})\})$ and $V^{(3)}(115) = V^{(3)}(\{(1,1,1),(2,2,2)\})$, four-site, $V^{(4)}(\{(1,1,1),(2,2,2),(3,3,3)\})$, and five-site $V^{(5)}(\{(1,1,1),(2,2,2),(3,3,3),(4,4,4)\})$ interactions.

It is important to note that such a straightforward connection to the concentration dependence of m_{Cr} cannot be made

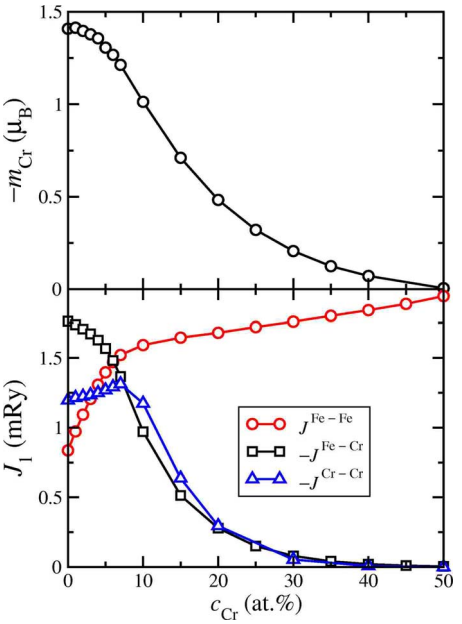

FIG. 11. (Color online) Upper panel: Local magnetic moment on Cr atoms m_{Cr}. Lower panel: Exchange interaction parameter J_1 of the magnetic Heisenberg Hamiltonian for different pairs of atoms in the FM state.

for the other ECI. However, the presence of anomalies can be clearly seen in the case of multisite interactions in Fig. 10. The picture is quite instructive: the concentration dependence of the ECI becomes stronger with increasing order of interactions. For instance, the five-site interaction $V^{(5)}(\{(1,1,1),(2,2,2),(3,3,3),(4,4,4)\})$ exhibits a pronounced maximum around 7 at % Cr in a very narrow concentration range. Such a behavior is suggestive of effects connected with the Fermi-surface topology changes, which indeed occur near that composition. Changes in the Fermi-surface topology are known to produce peculiarities, especially in the properties that are high order derivatives of the free energy with respect to external parameters.

The important point here is that such strongly concentration-dependent n-site interactions can be transformed into the concentration-independent form only through the interactions of even higher order, $n+m$, where m is the minimum degree of a polynomial that can fit the observed concentration dependence. From the results presented above it follows that finding an accurate concentration-independent cluster expansion for FM Fe-Cr alloys is a formidable task, as it requires taking into consideration high-order multisite interactions, in order to be able to capture the physical effects related to the Fermi-surface topology and its sudden changes with composition.

V. LOCAL ENVIRONMENT EFFECTS IN Fe-RICH ALLOYS

The results for ECI, presented in Sec. IV, have been obtained within the CPA, i.e., within the single-site mean-field approximation for the electronic structure of random alloys, which neglects local environment effects. From the previous discussion it is clear, however, that such effects must be very pronounced in the Fe-rich region due to frustrated magnetic exchange interactions of the Fe-Cr and Cr-Cr pairs. In order to investigate these effects, we have calculated the electronic structure and the effective interactions using a 432-atom supercell, which models a random $Fe_{87.5}Cr_{12.5}$ alloy. The calculations have been done by the LSGF method, with the local interaction zone that includes the nearest- and next-nearest-neighbor shells of atoms around each site in the supercell.

In Fig. 12 we show the magnetic moment (integrated over the atomic sphere) of Cr atoms, plotted as a function of the number of Cr atoms in the nearest-neighbor coordination shell. One can see that the dependence is very strong: the magnetic moment on Cr atoms changes linearly from $-1.5\mu_B$ to almost zero when the number of the nearest-neighbor Cr atoms increases from 0 to 4. This result is very similar to the result obtained by Klaver *et al.*[26] in the supercell projector augmented wave (PAW) calculations. This also means that Cr atoms having different local environments should also have different effective interactions with the Fe atoms.

In Fig. 13 we demonstrate the EPI at the first coordination shell obtained by SGPM for an inhomogeneous random alloy modeled by supercell LSGF calculations. The CPA effective medium in this case is built on the basis of all the atoms in the supercell. One can see that the interactions are very sensitive to the local environment of Cr atoms. In particular, there is a substantial drop of the interaction when the second Cr atom appears at the first coordination shell of the central Cr atom. We can also conclude from the results of our supercell calculations that local environment of Fe atoms plays less important role, at least for this particular alloy composition.

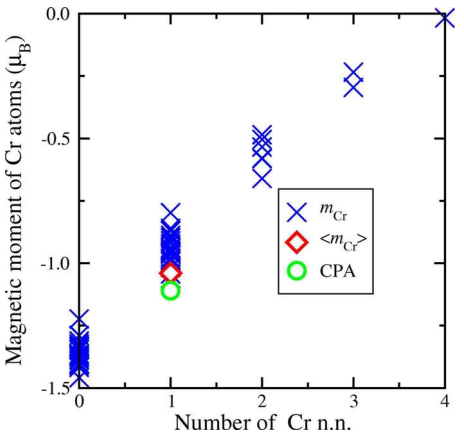

FIG. 12. (Color online) Magnetic moment of Cr atoms in random $Fe_{87.5}Cr_{12.5}$ alloy in the FM state as a function of the number of nearest-neighbor Cr atoms.

The obtained dependence of interactions on the local environment indicates that the usual Ising-type model of configurational energetics breaks down for Fe-rich Fe-Cr alloys in the FM state. The point is that there is no other way to represent the local environment effects in the model than to include the corresponding nine-site interactions directly in the Hamiltonian. An additional complication is that, as we have seen above for the FM state, the multisite interactions in the Fe-rich region become anomalously large and strongly concentration dependent due to changes of the Fermi-topology. It is then clear that an accurate *ab initio* description of the configurational energetics in the FM Fe-rich Fe-Cr alloys is a highly nontrivial problem. We will address this issue in a separate investigation. Here we would also like to note that, although the CPA completely neglects the local

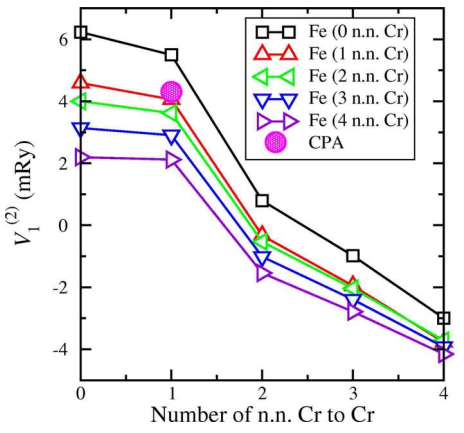

FIG. 13. (Color online) EPI at the first coordination shell for pairs Fe and Cr atoms with different numbers of Cr atoms in their first coordination shell ($Fe_{87.5}Cr_{12.5}$ alloy in the FM state).

environment effects, it yields quite accurate values for configuration-averaged quantities, such as local magnetic moments of Cr atoms (Fig. 12), as well as for the EPI. The latter is illustrated in Fig. 13: the CPA value coincides with the EPI for Fe and Cr atoms having one Cr atom at the first coordination shell, which is the average local environment in a random bcc $Fe_{87.5}Cr_{12.5}$ alloy.

VI. FINITE-TEMPERATURE MAGNETISM AND MAGNETIC ENERGETICS IN bcc Fe-Cr

Following the insightful works of Zener,[104] it has been generally recognized that any serious theoretical consideration of the phase equilibria in Fe-based alloys should take the magnetic (spin) degrees of freedom into account.[18–20,105–108] First of all, this concerns the ferromagnetic ordering transition, which causes a strong change of the thermodynamic properties near the Curie temperature. Therefore in the present paper we investigate this transition as a function of Cr concentration for Fe-rich Fe-Cr alloys.

As a starting point we assume that the magnetic configurational energy near the Curie temperature in these alloys is given by a classical Heisenberg Hamiltonian

$$H = -\sum_{ij}{}' J_{ij}^{(2)} \sigma_i \sigma_j, \tag{10}$$

where σ_i and σ_j are unit vectors in the directions of spin moments at sites i and j, respectively, and $J_{ij}^{(2)}$ is the exchange interaction parameter. Although the Heisenberg Hamiltonian assumes independence of the exchange interaction parameters on the magnetic state, this condition is rarely satisfied in real systems. In particular, for bcc Fe it was demonstrated, first by Heine *et al.*[109] and more recently by Ruban *et al.*,[42] that the exchange interactions differ substantially in ferromagnetic and paramagnetic states. This means that the exchange interactions are functions of the corresponding global magnetic state and, consequently, they must be temperature dependent.

Near the ferromagnetic ordering transition, which is a second-order phase transition, the global magnetic state may be considered to be close to the paramagnetic state, which, in turn, may be represented (in the mean-field consideration) by the homogeneous disordered-local-moment state. Therefore, we calculate the exchange interaction parameters relative to the DLM state using a perturbation-theory technique.[110] In these calculations we neglect the Fe-Cr and Cr-Cr magnetic interactions because the magnetic moments on Cr atoms vanish in the DLM state.[111] This result (disappearance of magnetic moments on Cr) feels somewhat artificial because it is obtained for a disordered magnetic state (DLM) considered at $T=0$. We note that local magnetic moments on Cr atoms appear quite naturally either as a result of ferromagnetic ordering or due to thermally induced longitudinal spin fluctuations at high temperatures. Nevertheless, in the present work, we consider that in Fe-rich Fe-Cr alloys the effect of these Cr moments on the ferromagnetic ordering transition is small relative to the leading contribution due to the Fe-Fe exchange interactions.

The statistical thermodynamic simulations of magnetic ordering have been performed by Monte Carlo method using a simulation box comprised of $12\times12\times12$ atoms (subject to periodic boundary conditions) distributed on sites of the bcc crystal lattice. A random distribution of Cr atoms in the supercell has been generated for each alloy composition in order to have a common well-defined chemical configurational state in all the considered cases. The Fe-Fe exchange interaction parameters have been calculated at a fixed lattice parameter of 2.87 Å. The calculated Curie temperatures are shown in Fig. 14, where they are compared to experimental values,[112–115] as well as with the concentration dependence of T_C adopted in the Calphad modeling.[21]

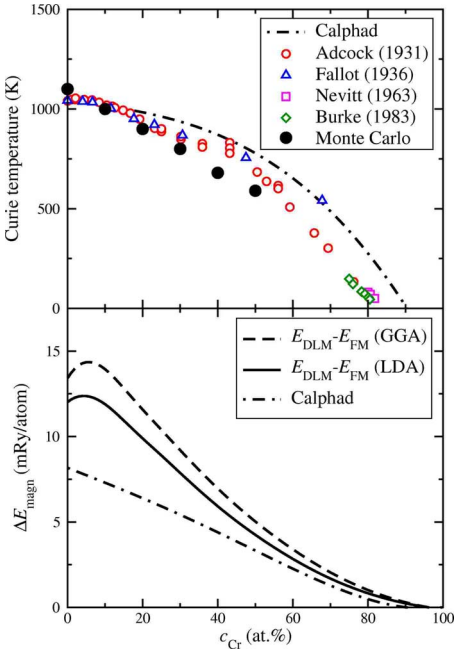

FIG. 14. (Color online) Upper panel: Critical (Curie) temperatures of magnetic ordering in the Fe-Cr system obtained in the present work using Monte Carlo simulations (full circles), in comparison with experimental results from Refs. 112–115 (open symbols) and with the compositional dependence used in Calphad modeling (Ref. 21) (dot-dashed line). Lower panel: Energy of magnetic ordering in the bcc Fe-Cr alloys, as calculated in the present work (solid line) and according to the Calphad description (Refs. 18 and 21) (dot-dashed line).

Figure 14 shows that our simulations reproduce the general trend of chromium to lower the Curie temperature of Fe-Cr alloys. However, we obtain an almost linear decrease in the Curie temperature with increasing the Cr content so that the experimentally reported[112,116,117] slight upturn of the T_C at small concentrations of Cr is not reproduced. This may be due to several factors unaccounted in our simulations. However, the most probable one is the influence of magnetic short-range order on the exchange interaction parameters, which, as discussed above, has been neglected in our calculations.

The point here is that the amount of magnetic short-range order is quite substantial near the Curie temperature. At the same time, as one can see from the lower panel of Fig. 14, there is a well-pronounced maximum on the first-principles energy difference between the ferromagnetic and DLM states, which originates entirely from the corresponding

TABLE III. The energy of magnetic ordering in bcc Fe, in units of the experimental Curie temperature $T_C=1043$ K. The theoretical results obtained using the GGA and LDA are compared with the Calphad representation of experimental information.

Source	$\Delta E_{\mathrm{magn}}/T_C$	Comment
Ref. 18	1.06	Calphad, from C_{magn}
This work	2.60	LDA, from J_0, DLM state
This work	1.82	LDA, as $E_{\mathrm{DLM}}-E_{\mathrm{FM}}$
This work	2.03	GGA, as $E_{\mathrm{DLM}}-E_{\mathrm{FM}}$

anomaly in the concentration dependence of the enthalpy of formation of random Fe-Cr alloys in the ferromagnetic state. This anomaly (see discussion in Sec. III B) is completely absent in the DLM state, in which the parameters of exchanges have been computed. At the same time, it should be present in the exchange interactions if one computes them starting from the FM state. Similarly, the anomaly should be present (although in a quite reduced form) in the interactions close to the critical point, which corresponds to the DLM state with a significant degree of ferromagnetic short-range order (SRO).

Let us finally comment on such an important thermodynamic quantity as the energy of magnetic ordering. This energy may be defined as

$$\Delta E_{\mathrm{magn}} = \int_0^\infty C_{\mathrm{magn}} dT, \tag{11}$$

where C_{magn} is a magnetic contribution to the heat capacity. The magnetic contribution was extracted from the experimental heat-capacity data for pure iron and selected Fe-Cr alloys by several authors,[105] and an analytic representation of these data was formulated within the Calphad modeling approach.[18,20,21,108] It is interesting to check whether consistency exists between the theoretically and experimentally derived energies of magnetic ordering.

The energy defined by Eq. (11) corresponds to the energy difference between the high-temperature disordered paramagnetic and completely ordered ferromagnetic states of the alloy. Within the simplest mean-field-like approach, the high-temperature paramagnetic state is presented by the disordered local-moment model. Therefore the energy of magnetic ordering in this case is $\Delta E_{\mathrm{magn}}=E_{\mathrm{DLM}}-E_{\mathrm{FM}}$. Our results for ΔE_{magn} obtained in the LDA and GGA for a fixed lattice parameter of 2.87 Å are presented in the lower panel of Fig. 14, where they are compared to the integrated magnetic heat-capacity contribution from Calphad. The obtained almost twofold difference between the calculated and the Calphad values for pure Fe is striking, taking into consideration that (1) there is very good agreement between theory and experiment for the magnetic transition temperature and (2) the Calphad value for pure iron is just a representation of the experimentally derived information.

In order to illuminate the problem further, we compare in Table III the magnetic ordering energy obtained by using different theoretical methods (Calphad value should be considered as experimental data). One can see that theoretical results are very sensitive to the model used in the calculations, but the worst agreement is found for the magnetic energy calculated from the exchange interaction parameters obtained in this work with respect to DLM state. Let us note that the result $\Delta E_{\mathrm{magn}}\approx(2-2.6)T_C$ is, nevertheless, very well consistent with the classical Heisenberg model. Within this model one gets $\Delta E_{\mathrm{magn}}=J_0$, where $J_0=\Sigma_j J_{0j}^{(2)}$ is the sum of magnetic exchange interactions over all distances. In the mean-field approximation $T_C^{\mathrm{mf}}=2/3J_0$.[118] Taking into account the well-known fact that the mean-field approximation overestimates the Curie temperature by about 30–45%, we arrive to the abovementioned result, namely, that the difference in ferromagnetic and paramagnetic energies is approximately equal to $(2-2.6)T_C$.

One reason why the same set of exchange interaction parameters gives the Curie temperature very accurately, but fails to reproduce the value of magnetic energy, is the fact that Fe cannot be accurately described by the classical Heisenberg model. Indeed, our calculations show that the magnetic exchange interactions in Fe are strongly dependent on the global magnetic state. Therefore, the interaction parameters, determined in this work for the paramagnetic DLM state, must be strongly renormalized in the completely ordered ferromagnetic state.[42] Direct total-energy calculations for both states, DLM and FM, give results that are closer to the Calphad or experimental ones. Still, the difference between experimental and theoretical magnetic energies is too large. As the energy of magnetic ordering is a key parameter for *ab initio* based modeling of phase transformations in iron and steel, this discrepancy calls for further theoretical investigations.

VII. SUMMARY

We have performed a detailed *ab initio* study of the electronic structure and physical properties of binary Fe-Cr alloys. In particular, we have calculated the cohesive properties of the alloys, the energies of chemical and magnetic interactions, and the local magnetic moments of Fe and Cr, as a function of concentration and magnetic state.

The properties of Fe-rich ferromagnetic alloys have been found to exhibit anomalous concentration dependencies. Two sources of these anomalies have been identified: (i) the appearance of local magnetic moments on Cr impurities in Fe-rich alloys and (ii) the change in Fermi-surface topology in the majority-spin channel at a composition of about 7 at % Cr. The calculated properties of Fe-Cr alloys in the paramagnetic DLM state exhibit no anomalies.

The established dependence of the effective interatomic interactions on the composition and magnetic state in Fe-Cr alloys is just one of the many complications to be dealt with when developing *ab initio* based atomistic models for the present alloy system. Another challenging problem is to develop a reasonably simple and accurate model for taking into account the longitudinal spin fluctuations, especially on Cr atoms at high temperature.[84,87] As what follows from our Monte Carlo results, these contributions may be important in order to reproduce the experimentally observed nonlinear

concentration dependence of the Curie temperature in the present system,[112,116] which, in turn, is important for obtaining an accurate description of the thermodynamics of Fe-Cr solid solution.[18] Coupling between the magnetic and structural degrees of freedom is of importance for modeling defects and structural phase transformations in steels.[87]

We would also like to draw attention to the obtained substantial difference between the first-principles results and Calphad data concerning the energy of magnetic ordering. The disagreement is alarming because the Calphad model for the magnetic contribution is based on many careful assessments of the existing experimental data while, on the other hand, the existing first-principles theories seem to reproduce other magnetic properties of 3*d* metals and their alloys quite accurately.

ACKNOWLEDGMENTS

This work was financed by the Swedish Foundation for Strategic Research (SSF) and by the Swedish Governmental Agency for Innovation Systems (VINNOVA). The computer resources for this study, at the Center for Parallel Computers (PDC), were provided by the Swedish National Infrastructure for Computing (SNIC). P.A.K. acknowledges financial support by the Swedish Nuclear Fuel and Waste Management Co. (SKB AB).

*Corresponding author; pavel@mse.kth.se
†Present address: Department of Materials Science and Engineering, Physical Metallurgy, Royal Institute of Technology, SE-100 44 Stockholm, Sweden.

[1] M. B. Cortie and H. Pollak, Mater. Sci. Eng., A **199**, 153 (1995).
[2] R. M. Fisher, E. J. Dulis, and K. G. Carroll, Trans. AIME **197**, 690 (1953).
[3] R. O. Williams and H. W. Paxton, J. Iron Steel Inst., London **185**, 358 (1957).
[4] M. Hillert, Sc.D. thesis, MIT, 1956.
[5] M. Hillert, Acta Metall. **9**, 525 (1961).
[6] J. W. Cahn, Acta Metall. **9**, 795 (1961).
[7] J. W. Cahn, Trans. Metall. Soc. AIME **242**, 166 (1968).
[8] J.-O. Nilsson, Mater. Sci. Technol. **8**, 685 (1992).
[9] The average composition of the steel specimen shown in Fig. 1 is 60.0% Fe, 30.9% Cr, 5.1% Ni, 2.8% Mo, 0.82% Mn, 0.34% Si, 0.007% C, and 0.059% N (weight percentage). The composition has been measured using the atom probe field ion microscopy (APFIM) technique.
[10] R. O. Williams, Trans. AIME **212**, 497 (1958).
[11] S. Katano and M. Iizumi, Phys. Rev. Lett. **52**, 835 (1984).
[12] J. C. LaSalle and L. H. Schwartz, Acta Metall. **34**, 989 (1986).
[13] S. M. Dubiel and G. Inden, Z. Metallkd. **78**, 544 (1987).
[14] F. Bley, Acta Metall. Mater. **40**, 1505 (1992).
[15] C. Lemoine, A. Fnidiki, F. Danoix, M. Hédin, and J. Teillet, J. Phys.: Condens. Matter **11**, 1105 (1999).
[16] Yu. I. Petrov, E. A. Shafranovsky, Yu. F. Krupyanskii, and S. V. Essine, J. Appl. Phys. **91**, 352 (2002).
[17] T. L. Swan-Wood, O. Delaire, and B. Fultz, Phys. Rev. B **72**, 024305 (2005).
[18] M. Hillert and M. Jarl, CALPHAD: Comput. Coupling Phase Diagrams Thermochem. **2**, 227 (1978).
[19] T. Nishizawa, M. Hasebe, and M. Ko, Acta Metall. **27**, 817 (1979).
[20] G. Inden, Physica B & C **103**, 82 (1981).
[21] J.-O. Andersson and B. Sundman, CALPHAD: Comput. Coupling Phase Diagrams Thermochem. **11**, 83 (1987).
[22] I. Cook, Nature Mater. **5**, 77 (2006).
[23] P. E. A. Turchi, L. Reinhard, and G. M. Stocks, Phys. Rev. B **50**, 15542 (1994).
[24] P. Olsson, I. A. Abrikosov, L. Vitos, and J. Wallenius, J. Nucl. Mater. **321**, 84 (2003).
[25] P. Olsson, I. A. Abrikosov, and J. Wallenius, Phys. Rev. B **73**, 104416 (2006).
[26] T. P. C. Klaver, R. Drautz, and M. W. Finnis, Phys. Rev. B **74**, 094435 (2006).
[27] M. Yu. Lavrentiev, R. Drautz, D. Nguyen-Manh, T. P. C. Klaver, and S. L. Dudarev, Phys. Rev. B **75**, 014208 (2007).
[28] A. V. Ruban, P. A. Korzhavyi, and B. Johansson, Phys. Rev. B **77**, 094436 (2008).
[29] I. A. Abrikosov, A. M. N. Niklasson, S. I. Simak, B. Johansson, A. V. Ruban, and H. L. Skriver, Phys. Rev. Lett. **76**, 4203 (1996).
[30] I. A. Abrikosov, S. I. Simak, B. Johansson, A. V. Ruban, and H. L. Skriver, Phys. Rev. B **56**, 9319 (1997).
[31] I. A. Abrikosov, Yu. H. Vekilov, P. A. Korzhavyi, A. V. Ruban, and L. E. Shilkrot, Solid State Commun. **83**, 867 (1992).
[32] P. A. Korzhavyi, A. V. Ruban, I. A. Abrikosov, and H. L. Skriver, Phys. Rev. B **51**, 5773 (1995).
[33] A. V. Ruban and H. L. Skriver, Phys. Rev. B **66**, 024201 (2002); A. V. Ruban, S. I. Simak, P. A. Korzhavyi, and H. L. Skriver, *ibid.* **66**, 024202 (2002).
[34] L. Vitos, Phys. Rev. B **64**, 014107 (2001); L. Vitos, I. A. Abrikosov, and B. Johansson, Phys. Rev. Lett. **87**, 156401 (2001).
[35] P. Soven, Phys. Rev. **156**, 809 (1967).
[36] B. L. Györffy, Phys. Rev. B **5**, 2382 (1972).
[37] J. S. Faulkner, Prog. Mater. Sci. **27**, 1 (1982).
[38] B. L. Györffy, A. J. Pindor, J. B. Staunton, G. M. Stocks, and H. Winter, J. Phys. F: Met. Phys. **15**, 1337 (1985).
[39] Y. Wang and J. P. Perdew, Phys. Rev. B **44**, 13298 (1991); J. P. Perdew, J. A. Chevary, S. H. Vosko, K. A. Jackson, M. R. Pederson, D. J. Singh, and C. Fiolhais, *ibid.* **46**, 6671 (1992).
[40] J. P. Perdew and Y. Wang, Phys. Rev. B **45**, 13244 (1992).
[41] I. Mirebeau, M. Hennion, and G. Parette, Phys. Rev. Lett. **53**, 687 (1984).
[42] A. V. Ruban, S. Shallcross, S. I. Simak, and H. L. Skriver, Phys. Rev. B **70**, 125115 (2004).
[43] F. Ducastelle and F. Gautier, J. Phys. F: Met. Phys. **6**, 2039 (1976).
[44] F. Ducastelle, *Order and Phase Stability in Alloys* (North-Holland, Amsterdam, 1991).
[45] G. D. Preston, Philos. Mag. **13**, 419 (1932).
[46] A. L. Sutton and W. Hume-Rothery, Philos. Mag. **46**, 1295 (1955).

[47] V. L. Moruzzi, J. F. Janak, and K. Schwarz, Phys. Rev. B **37**, 790 (1988).
[48] P. A. Korzhavyi, A. V. Ruban, S. I. Simak, and Yu. Kh. Vekilov, Phys. Rev. B **49**, 14229 (1994).
[49] G. R. Speich, A. J. Schwoeble, and W. C. Leslie, Metall. Trans. **3**, 2031 (1972).
[50] J. T. Lenkkeri, J. Phys. F: Met. Phys. **10**, 611 (1980).
[51] E. E. Lähteenkorva and J. T. Lenkkeri, J. Phys. F: Met. Phys. **11**, 767 (1981).
[52] D. I. Bolef and J. de Klerk, Phys. Rev. **129**, 1063 (1963).
[53] W. A. Dench, Trans. Faraday Soc. **59**, 1279 (1963).
[54] L. Pauling, *The Nature of the Chemical Bond* (Cornell University Press, New York, 1960).
[55] W. Hume-Rothery, J. Inst. Met. **35**, 295 (1926); W. Hume-Rothery and G. V. Raynor, *The Structure of Metals and Alloys* (Institute of Metals, London, 1954).
[56] H. Jones, Proc. Phys. Soc. London **49**, 250 (1937); J. Phys. Radium **23**, 637 (1962).
[57] T. B. Massalski and U. Mizutani, Prog. Mater. Sci. **22**, 151 (1978).
[58] D. G. Pettifor, in *Physical Metallurgy*, 4th ed., edited by R. W. Cahn and P. Haasen (North-Holland, Amsterdam, 1996), Vol. 1, pp. 47–133.
[59] I. M. Lifshitz, Zh. Eksp. Teor. Fiz. **38**, 1569 (1960) [Sov. Phys. JETP **11**, 1130 (1960)].
[60] V. S. Egorov and A. N. Fedorov, Zh. Eksp. Teor. Fiz. **85**, 1647 (1983) [Sov. Phys. JETP **58**, 959 (1983)].
[61] V. G. Vaks and A. V. Trefilov, J. Phys. F: Met. Phys. **18**, 213 (1988).
[62] A. A. Varlamov, V. S. Egorov, and A. V. Pantsulaya, Adv. Phys. **38**, 469 (1989).
[63] M. I. Katsnelson, I. I. Naumov, and A. V. Trefilov, Phase Transitions **49**, 143 (1994).
[64] Ya. M. Blanter, M. I. Kaganov, A. V. Pantsulaya, and A. A. Varlamov, Phys. Rep. **245**, 159 (1994).
[65] E. Bruno, B. Ginatempo, E. S. Giuliano, A. V. Ruban, and Yu. Kh. Vekilov, Phys. Rep. **249**, 353 (1994).
[66] N. I. Kulikov and C. Demangeat, Phys. Rev. B **55**, 3533 (1997).
[67] E. A. Smirnova, P. A. Korzhavyi, Yu. Kh. Vekilov, B. Johansson, and I. A. Abrikosov, Phys. Rev. B **64**, 020101(R) (2001); Eur. Phys. J. B **30**, 57 (2002).
[68] A. T. Paxton, M. Methfessel, and D. G. Pettifor, Proc. R. Soc. London, Ser. A **453**, 1493 (1997).
[69] J. S. Faulkner and G. M. Stocks, Phys. Rev. B **21**, 3222 (1980).
[70] B. L. Györffy and G. M. Stocks, J. Phys. F: Met. Phys. **10**, L321 (1980).
[71] It should be noted here that density-functional theory (DFT)–based calculations normally predict the hole arms along the H-N-H direction to be connected (Refs. 72–75), whereas experimentally they are found to be disrupted (Refs. 76–78) near point N.
[72] J. Callaway and C. S. Wang, Phys. Rev. B **16**, 2095 (1977).
[73] W. B. Johnson, J. R. Anderson, and D. A. Papaconstantopoulos, Phys. Rev. B **29**, 5337 (1984).
[74] J. Schäfer, M. Hoinkis, E. Rotenberg, P. Blaha, and R. Claessen, Phys. Rev. B **72**, 155115 (2005).
[75] A. Grechnev, I. Di Marco, M. I. Katsnelson, A. I. Lichtenstein, J. Wills, and O. Eriksson, Phys. Rev. B **76**, 035107 (2007).
[76] D. R. Baraff, Phys. Rev. B **8**, 3439 (1973).
[77] R. V. Coleman, W. H. Lowrey, and J. A. Polo, Jr., Phys. Rev. B **23**, 2491 (1981).
[78] T. Nautiyal and S. Auluck, Phys. Rev. B **32**, 6424 (1985).
[79] http://www.phys.ufl.edu/fermisurface/
[80] T.-S. Choy, J. Naset, J. Chen, S. Hershfield, and C. Stanton, Bull. Am. Phys. Soc. **45**(1) L3642 (2000).
[81] A. V. Ruban and H. L. Skriver, Phys. Rev. B **55**, 8801 (1997).
[82] L. Vitos, P. A. Korzhavyi, and B. Johansson, Phys. Rev. Lett. **88**, 155501 (2002).
[83] L. Vitos, P. Korzhavyi, and B. Johansson, Nature Mater. **2**, 25 (2003).
[84] G. Grimvall, J. Häglund, and A. Fernández Guillermet, Phys. Rev. B **47**, 15338 (1993).
[85] S. Shallcross, A. E. Kissavos, V. Meded, and A. V. Ruban, Phys. Rev. B **72**, 104437 (2005).
[86] A. V. Ruban, S. Khmelevskyi, P. Mohn, and B. Johansson, Phys. Rev. B **75**, 054402 (2007).
[87] L. Vitos, P. A. Korzhavyi, and B. Johansson, Phys. Rev. Lett. **96**, 117210 (2006).
[88] L. D. Landau and E. M. Lifshitz, *Quantum Mechanics* (Pergamon, Oxford, 1977).
[89] M. Hennion, J. Phys. F: Met. Phys. **13**, 2351 (1983).
[90] P. E. A. Turchi, M. Sluiter, and G. M. Stocks, *High Temperature Ordered Intermetallic Alloys IV*, edited by L. Johnson, D. P. Pope, and J. O. StieglerMRS Symposia Proceedings No. 213 (Materials Research Society, Pittsburgh, 1991), p. 75.
[91] L. Reinhard, J. L. Robertson, S. C. Moss, G. E. Ice, P. Zschack, and C. J. Sparks, Phys. Rev. B **45**, 2662 (1992).
[92] G. J. Ackland, D. J. Bacon, A. F. Calder, and T. Harry, Philos. Mag. A **75**, 713 (1997).
[93] B. J. Lee, M. I. Baskes, H. Kim, and Y. K. Cho, Phys. Rev. B **64**, 184102 (2001).
[94] M. I. Mendelev, S. Han, D. J. Srolovitz, G. J. Ackland, D. Y. Sun, and M. Asta, Philos. Mag. **83**, 3977 (2003).
[95] P. Olsson, J. Wallenius, C. Domain, K. Nordlund, and L. Malerba, Phys. Rev. B **72**, 214119 (2005); **74**, 229906(E) (2006).
[96] S. L. Dudarev and P. M. Derlet, J. Phys.: Condens. Matter **17**, 7097 (2005).
[97] G. J. Ackland, J. Nucl. Mater. **351**, 20 (2006).
[98] P. M. Derlet and S. L. Dudarev, Prog. Mater. Sci. **52**, 299 (2007).
[99] G. Liu, D. Nguyen-Manh, B.-G. Liu, and D. G. Pettifor, Phys. Rev. B **71**, 174115 (2005).
[100] R. Drautz and D. G. Pettifor, Phys. Rev. B **74**, 174117 (2006).
[101] A. T. Paxton and M. W. Finnis, Phys. Rev. B **77**, 024428 (2008).
[102] A. V. Ruban and I. A. Abrikosov, Rep. Prog. Phys. **71**, 046501 (2008).
[103] The same is true of Cr atoms; they gain nonzero average magnetic moments and as a result thermally induced longitudinal spin fluctuations. However, these moments are relatively small. Therefore, we hope that the relative error due to the neglect of longitudinal spin fluctuations is also small. On the other hand, at present, there is no consistent first-principles theory which can treat spin fluctuations in alloys.
[104] C. Zener, Trans. AIME **203**, 619 (1955).
[105] R. J. Weiss and K. J. Tauer, Phys. Rev. **102**, 1490 (1956).
[106] V. Heine and R. Joint, Europhys. Lett. **5**, 81 (1988).
[107] G. Grimvall, Phys. Rev. B **39**, 12300 (1989).
[108] D. de Fontaine, S. G. Fries, G. Inden, P. Miodownik, R. Schmidt-Fetzer, and S. L. Chen, CALPHAD: Comput. Coupling Phase Diagrams Thermochem. **19**, 499 (1995).

[109] V. Heine, A. I. Lichtenstein, and O. N. Mryasov, Europhys. Lett. **12**, 545 (1990).
[110] A. Liechtenstein, M. I. Katsnelson, and V. A. Gubanov, J. Phys. F: Met. Phys. **14**, L125 (1984); A. Liechtenstein, M. I. Katsnelson, V. P. Antropov, and V. A. Gubanov, J. Magn. Magn. Mater. **67**, 65 (1987).
[111] J. Kübler, *Theory of Itinerant Electron Magnetism* (Clarendon, Oxford, 2000), p. 323.
[112] F. Adcock, J. Iron Steel Inst., London **124**, 99 (1931).
[113] M. Fallot, Ann. Phys. (Paris) **6**, 305 (1936).
[114] M. V. Nevitt and A. T. Aldred, J. Appl. Phys. **34**, 463 (1963).
[115] S. K. Burke, R. Cywinski, J. R. Davis, and B. D. Rainford, J. Phys. F: Met. Phys. **13**, 451 (1983).
[116] G. Kirchner, T. Nishizawa, and B. Uhrenius, Metall. Trans. **4**, 167 (1973).
[117] L. Nylöf, AB Sandvik Materials Technology Research & Development Technical Report No. 070059TE, 2007 (unpublished).
[118] D. B. Downie and J. F. Martin, J. Chem. Thermodyn. **16**, 743 (1984).